



# GIS-Based AHP and FR Methods for Landslide Susceptibility Mapping in the Abay Gorge, Dejen–Renaissance Bridge, Central, Ethiopia

Chalachew Tesfa

Received: 27 March 2022 / Accepted: 20 May 2022 / Published online: 27 June 2022  
© The Author(s), under exclusive licence to Springer Nature Switzerland AG 2022

**Abstract** The study area is situated in the Abay Gorge near Dejen, in Central Ethiopia. The place is affected by landslides, roadside slides, and further road failures. This study provides a detailed evaluation of causative factors for landslides, characterizes the materials on slopes, and assesses the hydrogeological condition of the study area. GIS techniques were employed to produce a zonation map for a landslide by combining the analytical hierarchy process (AHP) and frequency ratio (FR) methods. The prepared landslide hazard zonation map of the area using AHP and FR approaches is classified further into five susceptibility classifications: extremely low (6 & 20%), low (26 & 20%), moderate (3 & 21%), high (20 & 20%), and very high (12 & 19) of AHP and FR respectively. In this study, the causes of the landslide were identified and included slope, aspect, rainfall, land use/cover, elevation, lithology, distance to streams, and distance to the road were analyzed. The results show that the landslides in the area were triggered by heavy rainfall. The fragile nature of the geological materials and heavy stream discharge aggravates the instability of the area. Accordingly, the following solutions are suggested: (1) constructing slope-retaining structures, (2) designing an adequate drainage system for road corridors (3) Encourage afforestation in the affected

areas, and (4) Using stream and drainage management practices to reduce flooding.

**Keywords** Characterization · Inventory · Causative factors · Road failures · Abay Gorge · Ethiopia

## 1 Introduction

Landslides are one of the key reasons resulting in the downhill movement of rock, soil, artificial fill, or a combination along slopes (Brunsdon and Thornes 1979 ; Varnes 1984; Cruden 1991). Landslides are the primary and the most natural disasters in both developing and developed countries in mountainous regions (Lee 2005; Tesfa and Woldearegay 2021). Mass wastings are geomorphological processes that affect the landscape and cause a variety of disruptions (Dahoua et al. 2017a). Geohazards, which are resulting from mass wasting are a major problem globally, including in many parts of Ethiopia. Therefore, it is important to study and identify the triggering mechanisms to enable the design of mitigation measures. Many studies (Dai et al. 2002; Ayalew and Yamagish 2005; Hagos 2013; Woldearegay 2013; Gautam et al. 2021; Manchar et al. 2018; Ye et al. 2022) have done on landslides in many parts of the world, including in Ethiopia.

Road transportation is important for sustainable economic and social development in many countries, especially in developing countries like Ethiopia.

C. Tesfa (✉)  
Debre Markos University, P. O. Box 269, Debre Markos,  
Ethiopia  
e-mail: chalachew\_tesfa@dmu.edu.et

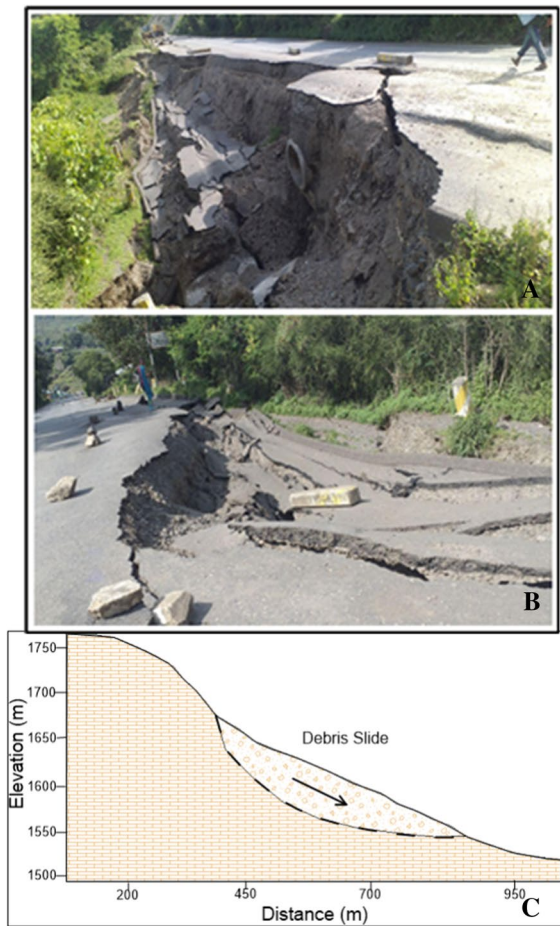
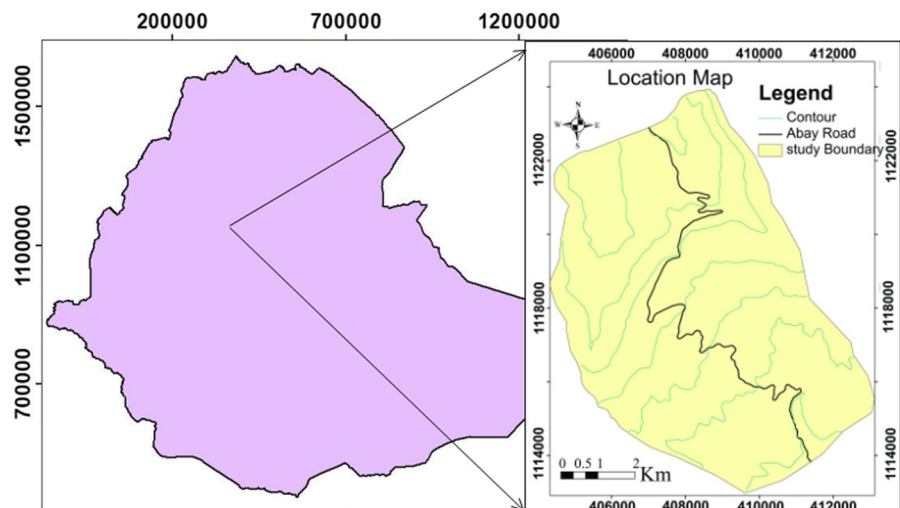


**Fig. 1** A photograph A, B showing an example of recent landslides and C. is a sketch of the slope failure mechanism at the selected sites along the Dejen to Renaissance bridge road section

**Fig. 2** Location Map of the area



Since Ethiopia's economic growth is highly dependent on the agricultural sector, suitable road infrastructures are needed for industrial and agricultural development Fig. 1.

The Abay Gorge area in Central Ethiopia is frequently affected by road failures. Especially the section of the road from Dejen to Renaissance Bridge is prone to landslides compared to the section from Goha -Tsion to Renaissance bridge (Fig. 2).

The roadside regions are affected by road failures, dislocations of farmlands, and different landforms. The Ethiopian Roads Authority (ERA) provides budgets for the maintenance of roads in the affected regions (Figs. 6A and 9A). This road is important because it links the capital city, Addis Ababa with the northwestern parts of the country (Fig. 2). It is also the main truck for the import and export of goods to Sudan. Disasters can be prevented or mitigated if they are predicted during development planning (Hadji et al. 2014). Therefore, it is important to study the causes of landslides, and road failures to minimize the effects on natural environments, agricultural land, and infrastructure. The landslides and road failures are one of the effects for delaying the transportation of raw and processed materials to markets. Hence it needs considerable attention and a detailed study to come up with a solution to the stated problems (Fig. 1A, B).

Landslide susceptibility mapping with GIS and quantitative methodologies is a popular method nowadays (Tang et al. 2020). Due to the advancement of remote sensing techniques, GIS plays a significant

role in the classification of different triggering factors of landslides and in identifying the past landslides to prepare a landslide inventory map (Zhao et al. 2022). It has become very easy to use data in the GIS to produce landslide susceptibility maps (Zhao et al. 2022). The frequency ratio (FR) and other statistical techniques based on GIS performed well with high accuracy (Mersha and Meten 2020). These are easy to use and can calculate how much each causative factor class contributes to the occurrence of landslides. The analytic hierarchy process (AHP) method was also used to determine the weights of the causal elements (Salehpour Jam et al. 2021; Das et al. 2022). Landslide susceptibility mapping (LSM) detects landslide-prone locations by correlating the significant landslide causalities with previous occurrences (Roccati et al. 2021).

## 2 General Settings

The location of the study area is found in the East Gojjam zone at the Abay Gorge (Fig. 2). Geographically, it is bounded by UTM coordinates of 1113000 m to 1,124,100 m North and 405,000 m to 414,000 m East. The climatic condition of the area is categorized as semi-Kolla which receives an average annual rainfall of 1250 mm recorded during the rainy period (Ethiopian Meteorological Agency). The temperature ranges from 25 to 30 °C. The elevation ranges from 1030 to 2451 a.m.s.l. The study area is accessible by an asphalt road that connects mainly the two large cities, Addis Ababa with Bahir Dar (Fig. 2).

The area is underlain by volcanic and sedimentary rock units. that comprise Basalt, Limestone with Gypsum intercalations, Siltstone with Shell intercalations, and Sandstone units (Fig. 3). The nature of the underlying geology and geomorphology of one area can be a primary driving agent for the occurrences of landslides and landslide-related vulnerabilities in the area (Barsch and Caine 1984; Hadji et al. 2013). The lithological units of the study area are described below.

### 2.1 Basaltic Units

This unit is largely deposited at the entrance of the gorge around the Dejen side and is characterized by massive, highly jointed columnar basalts exposed at

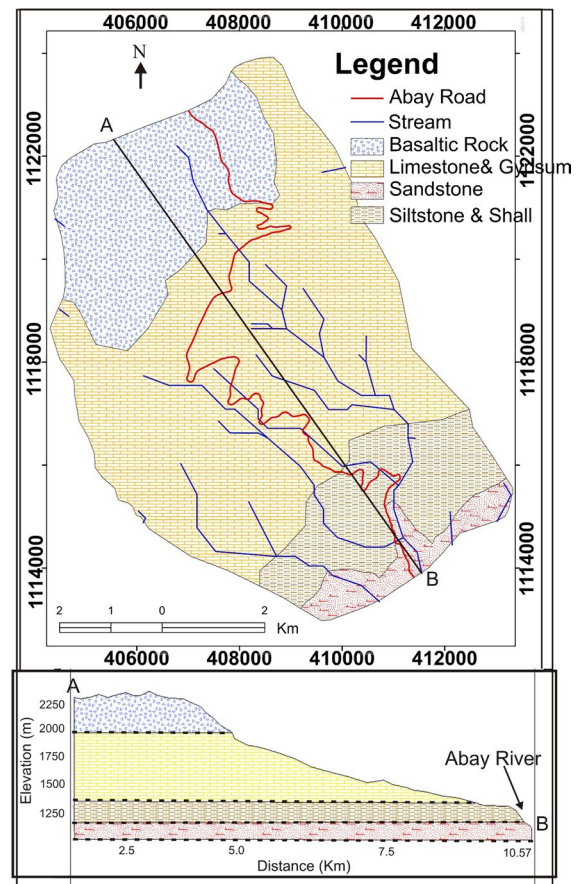


**Fig. 3** Lithological maps with the cross-sectional view

the top, cliffside, and roadsides. The total thickness of the basaltic rock was recorded to be 340 m with showing cracked and detached jointed rocks that fall at the lower bottom and cover the stream which passed under it. Generally speaking, the rockfalls are the main problems that are observed in this lithologic unit becoming unstable due to vertical slope and erosion which eventually cause the falling of rock fragments under gravity. Due to its topography (gravity), and nature of the material the rockfalls in this lithologic unit travel long-distance and faster movements.

### 2.2 Limestone & Gypsum

This unit is covering a large part of the study area compared with others. It covers a total thickness of 1 km and is characterized by unconsolidated fractured materials of marl-shale and relatively stable limestone beds (Fig. 3). The beds of limestone units are covered

by some unconsolidated and transported materials of the marl-shale with an average bedding thickness of 0.5 m. At the contact part between limestone and sandstone, the gypsum materials are exposed to the surface as road cut and river cut exposures at the bottom of limestone material. The gypsum unit consists of a thinly bedded with an average thickness of 15 to 25 cm alternative interval with limestone and gypsum beds. In some parts, quarry sites are observed for gypsum material mining for industrial and other purposes. Debris slides generally occur at this lithology that caused damage to areas along the valleys, roads, and farmlands. In general, this unit is the most prevalent type of instability in the area.

### 2.3 Siltstone & Shale

This unit is exposed at the road cut, hillside, and river cut exposures. In most parts, this unit shows weathered and altered nature in the lower parts of the gorge. For the most part, this unit shows weathered light red colors. In some parts, the grains of this unit are larger and show a lamination structure (Fig. 3).

### 2.4 Sandstone

This lithologic unit is exposed in the southern part of the study area at the river beds and abutments of the Abay River. This unit shows cemented nature with silica materials. Due to this nature shows a better strength than the siltstone and shall unit. The grains are shown sub-rounded to angular in shape, fine to coarse in size, and compositionally dominated by quartz, feldspar, plagioclase, and iron minerals. The estimated exposed thickness is about 20 m, as can be seen from the road cut exposures towards the Abay river cut at the bridge. Sedimentary structures like bedding planes and laminations are common in this lithologic unit.

The hydrogeological conditions of the study area were highly characterized by stream and river discharges. The groundwater condition was measured by groundwater discharge measurement techniques at the stream discharge areas. The correlation between groundwater and precipitation is investigated from the record of the rain gauges installed in the Abay Gorge and Dejen area and the mean annual rainfall is 1200 mm.

The area receives rainfall intensively, 600–700 mm, for two months that is in July and August the rainy season of the country. This level of rainfall is most suitable for deep percolation and leads to the groundwater increase (recharged) and then the pore water pressure increase. As a result, shear resistance decreases and finally triggered a landslide in the area Fig. 4.

## 3 Methods and Approaches

### 3.1 Landslide Inventory

A landslide inventory was produced based on a detailed field survey, google earth image explanations (Fig. 5) furthermore the selected eight landslide causative factor maps of the slope, aspect, elevation, land-use/ cover, rainfall, lithology, distance from the river, and road maps were prepared, that later utilized for FR and AHP approaches and the susceptibility map preparation (Fig. 4). Then, the prepared landslide susceptibility map was validated with the existing landslide areas (Inventories) by overlaying on

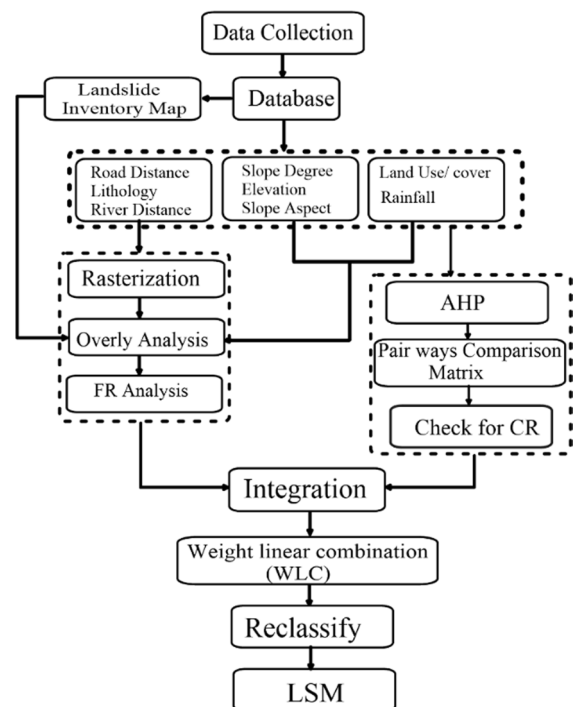


**Fig. 4** The flow chart shows the approach to study

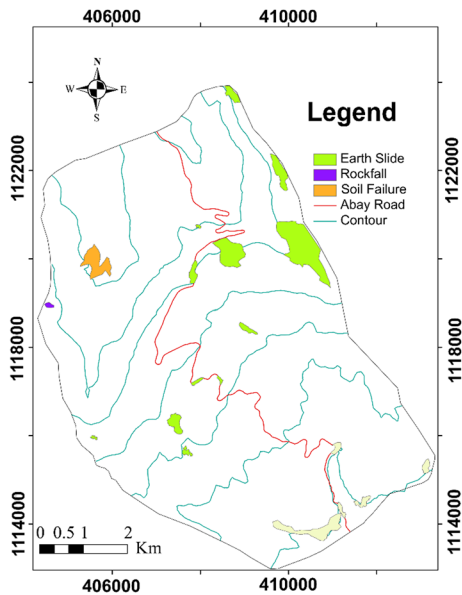


**Fig. 5** Inventory Map of the study area

each other with percentages of its coverage and also to checkup the relationships of the two approaches, through the area under the curve (AUC) application (Lee 2005) using Microsoft Excel software. For spatial data management, the Geographic Information System (GIS) is the primary instrument (Tang et al. 2020). Finally, the produced LSM has been classified into five landslide susceptibility classes very low, low, moderate, high, and very high susceptibility. There are many landslide susceptibility assessment methods, for this study Analytical hierarchy processes (AHP) and frequency ratio (FR) were selected (Fig. 4).

### 3.2 Analytical Hierarchy Process (AHP)

Is a multi-criteria decision-making process of measurement through pairwise comparisons and relies on the judgments of the experts to derive priority scales (Tesfa and Woldearegay 2021). The AHP operates at four levels defining the problem, determination of goals and alternatives, constructing of pairwise comparison matrix, constructing a normalizing Pair-wise comparison matrix, defining criteria weights, and gaining general priority (Dahoua et al. 2017a). In landslide susceptibility mapping, different landslide causative factors are considered as alternatives.

### 3.3 Frequency Ratio (FR)

The FR is a variation of the probabilistic model and is based on the observed relations between the distribution of landslides and the correlated causative factors (Tesfa and Woldearegay, 2021). The frequency ratio method is an applied method to determine the level of correlation between the location of the landslides in the study area and the causative factors (Solaimani et al. 2013), and the approach operated at the following stages. The consistency index, (CI) is calculated as (Eq. 1) below:

$$CI = (\lambda \max - n)/(n - 1) \tag{1}$$

where  $\lambda \max$  is the maximum eigenvalue in the matrix.  $n$  is total factors. CI can be compared with that of a random matrix, RI. The ratio from CI/RI is the consistency ratio, CR (Eq. 2). According to (Saaty, 2000) the value of CR should be less than 0.1.

$$CR = CI/RI \tag{2}$$

where RI is the average consistency index based on the order of the matrix (Saaty, 2000). According to (Voogd, 1988) LSI is calculated by using Eq. 3 below.

$$LSI = \sum_{i=1}^n (Wj * Wij) \tag{3}$$

where LSI is the landslide susceptibility index,  $Wj$  is the weight value for parameter  $j$ ,  $Wij$  is the rating/weight value for class  $i$  of parameter  $j$ , and  $n$  is parameter/ factor numbers. Finally, the LSI was created by summing the FR values (Eq. 5) in the conventional FR method (Eq. 4).

$$FR = \frac{\% \text{ of landslides in each class of parameter}}{\% \text{ of area pixels in the related class}} \tag{4}$$

The calculated weights are sum-up together in GIS and the produced map is subdivided into four zones.

$$LSI = \sum_{i=1}^n FR \tag{5}$$

where FR is the obtained frequency ratio of each factor;  $n$  is the factor numbers.

### 3.4 Landslide Causative Factors

According to several researchers, different landslide causative factors can encourage the occurrence of landslides in an area. For this research work slope, aspect, rainfall, land use/cover, elevation, lithology, distance to streams, and distance to the road were selected for further analysis with the selected landslide susceptibility analysis models. The selected eight causative factors were 30\*30 m resolutions.

### 3.5 Landslide Susceptibility Analysis

All the selected landslide causative factors were based on their influencing factor weight by using the selected two models of FR and AHP in the GIS windows for each landslide susceptibility index (LSI).

### 3.6 Validation Methods

The validation of produced landslide susceptibility maps produced by using AHP and FR models were verified by cross-checking with overlaying the existing landslide locations on the produced landslide inventories. Using the cut-off values, the landslide susceptibility map generated based on prescribed weight values using the Weight of Evidence approach was split into four groups: low, medium, high, and extremely high. The ROC curve generated from all landslides, including the modeling and validation sets, was used to categorize them.

In this study, the investigator identified that most produced landslide susceptibility maps fall in both very high and high susceptible zones of the inventory areas and hence it can be concluded that the selected model and the result were effective for landslide susceptibility zonation mapping of the work.

## 4 Results

### 4.1 Inventory Mapping

The landslide inventory map was made by identifying past landslide history location, extent, and type of landslides observed in the area (Fig. 5). Landslide areas were determined by analyzing aerial photos and field observations (Hadji et al. 2013). Therefore, the inventory provides useful information about the

probable occurrences of potential landslides in the future (Asmare and Tesfa 2022). Landslide inventory data were collected through detailed fieldwork/investigations using hand GPS and Google Earth image interpretation which includes the size, location, type, and extent of the recorded landslides, and finally digitized as a polygon in Arc GIS (Dahoua et al. 2017b). The field survey and gathering information was performed mainly to collect all relevant information about the past landslides, geological environments, geological structures, river/streamflow, and groundwater occurrences and to confirm/modify the various factor maps prepared during the pre-fieldwork phase. The occurrence of slope failure is caused by geologic, geomorphologic, rainstorm, and anthropogenic factors (El Mekki et al. 2017). For past landslides, an inventory map was systematically prepared using GPS. The possible fault mechanisms, type of slope materials, presence of shallow / groundwater, and possible triggers were collected. More than nineteen active and past landslide inventories were recorded, Earth slides, rockfalls, and soil embankment failures were the major ones. Several factor maps (elevation, slope, rainfall, lithology, road distance, watercourse distance, aspect, and the land use/cover), which were then used for landslide risk analysis, were produced by using Google Earth images, topographical maps (1:50,000), DEM (30×30 m), and hand GPS Fig. 6.

### 4.2 Landslide Causative Factors of the Area

#### 4.2.1 Slope Degree

The degree of the slope area was prepared by using DEM (30 m by 30 m) and classified into five slope subclasses based on the degree of slope. For the present work, the slope is defined by steep features, cliffs, and steep slopes and becomes smooth towards the tip. In general, steep slopes are more vulnerable to instability than gentle slopes (Hamza and Raghuvanshi 2017). The study area slope subclass is 0–10, 10–20, 20–30, 30–40 and > 40 (Fig. 7a).

#### 4.2.2 Slope Aspect

The aspect of the slope refers to the way the slope is facing. Consequently, it has an important contribution to the erosion of hilly rocks. The slope aspect of the zone was also prepared by using DEM (30 m



**Fig. 6** Photographs showing maintenance of the **A** roadsides slides, and **B** rock slides

by 30 m) and then classified into nine subclasses as planes (–1), north (0–22.5), north-east (22.5–67.5), east (67.5–112.5), southeast (112.5–157.5), south (157.5–202.5), southwest (202, 5–247.5), west (247.5–292.5) and northwest (292.5–360) as shown in (Fig. 7b).

#### 4.2.3 Elevation

The study area was a part of central Ethiopian highlands, and its elevation ranges from 1,030 m to 2451 m recorded at renaissance bridge and Dejen respectively (Fig. 7c). The elevation was subdivided into five classes 1030–1368, 1368–1603, 1603–1848, 1848–2158, 2158–2451 m.a.s.l. The maximum and minimum elevations within this specific area were about 2451 m and 1030 m. Landslide distributions in the sub-divided areas of elevation according to FR are 1368–1603, and 1603–1884 m which occurred at the minimum and maximum respectively (Fig. 7c).

#### 4.2.4 Land Use/Cover

The land use/land cover map was prepared by using Landsat 30 m and then classified into seven classes

cultivated land, forest land, meadow, shrub, water-body, artificial surface, and bare land (Fig. 7d). Finally converted into shapefile and exported to Arc GIS. The main area was enclosed by cultivated land and grassland. The frequency of landslides was commonly observed in the cultivated land class (Fig. 7d).

#### 4.2.5 Lithology

The lithology map of the area was produced at a scale of 1:50,000, and most of the study area was covered with sandstone, gypsum unit, limestone, basalt, and quaternary deposits. (Fig. 7e). Since the geological units have considerable variations in terms of strength, composition, and hydraulic property, the lithology contributed to the presence of landslides in an area. The lithology was complicated, hard, and soft rocks, including soil/deposits, are observed. These materials consist of rock fragments and soil, which were accumulated on the slopes.

#### 4.2.6 Distance to Stream

The stream distance map shows the occurrence of surface and subsurface water in the area. Similarly, it indicates the weak zones and shear zones following the streams and gully erosion of the area. The geological units were eroded by the tributaries of the Abay river and gully erosions that were formed by intense rainfalls can also be the cause of the slope instability due to internal erosions. Stream distance was prepared from the topographical map and then edited by using Arc GIS (Fig. 7f).

#### 4.2.7 Distance to Road

According to (Mittal et al. 2008) critical slope grades for highway construction cause vibrations by vehicles, and encourage landslide occurrences. Frequent landslides were observed on the sides of the road cut exposures consecutively highlighting the means that the road cut may be unstable or the road vibrations by vehicles induced landslides in the area. Construction of roads besides sloppy terrain results in some tensions, load decreasing on the slope heels, and landslides may happen eventually (Ayalew and Yamagishi 2005). Therefore, the road proximity to the landslide area was considered a causative factor (Fig. 7g).

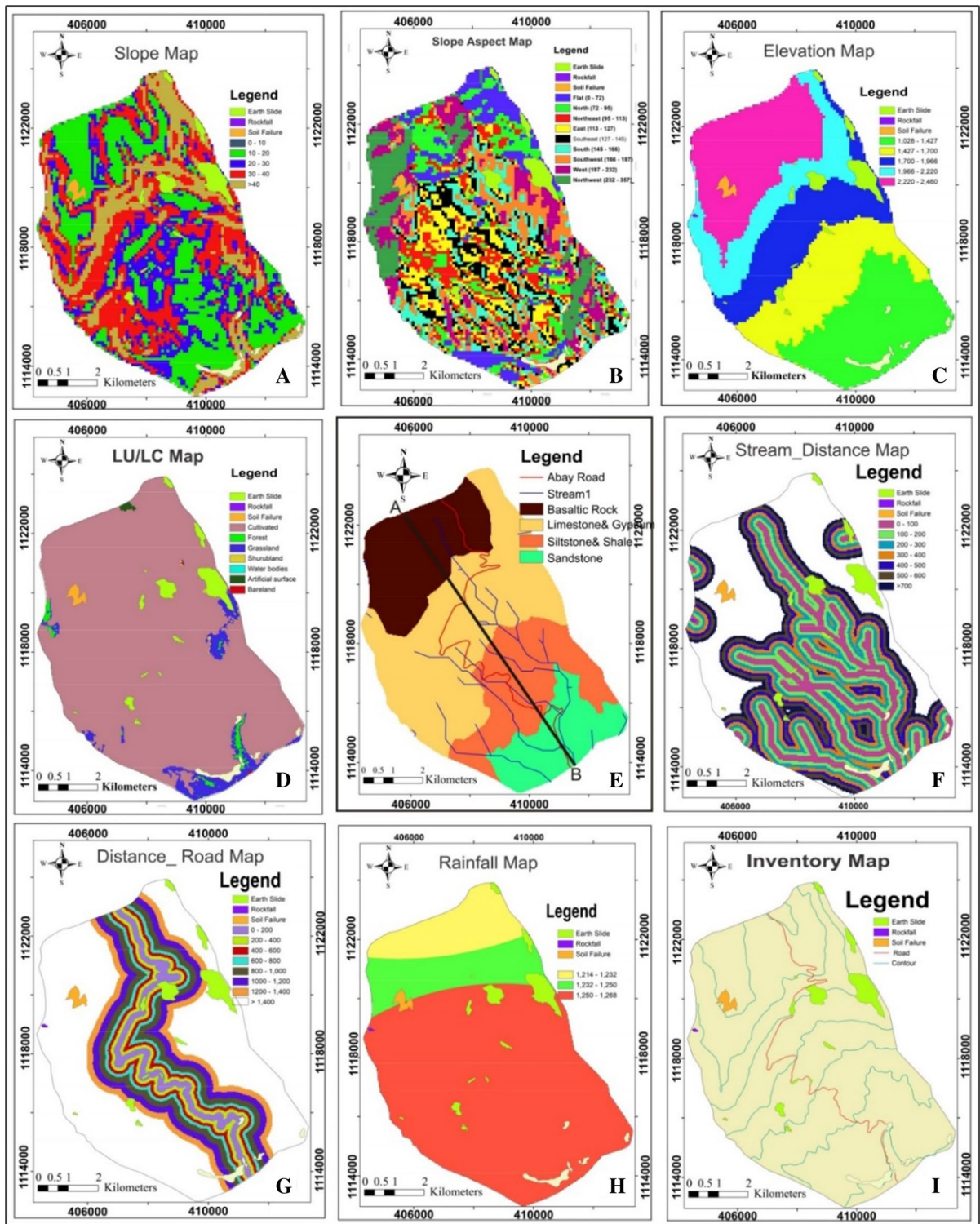


Fig. 7 Landslide causative factor map of the study



#### 4.2.8 Rainfall

Rainfall was a major issue initiation for the occurrence of geohazards (Hamad et al. 2018) due to its significant influence on the runoff and porewater pressure. The average monthly precipitation data were obtained from two existing weather stations for the past twenty years (2000 to 2020). The stations are located at Dejen and Abay Sheleko average yearly precipitation of 1211.8–1170 mm, respectively, and the daily temperature of the area varies from 25 to 31 °C. An annual rainfall map of the study area was prepared with an inverse distance weighting (IDW) method (Fig. 7h).

### 4.3 Landslide Susceptibility Mapping

#### 4.3.1 Landslide Susceptibility Map by Frequency Ratio (FR)

The frequency ratio was one of the most typically used techniques in the statistical evaluation of landslide investigation, which was the experimental relationship between the geo-hazards of each and all causal outcomes for landslides at the place. Subsequently, this approach established the spatial relationships between the available landslide and the descriptive effect of the landslide (Lee 2005). This technique calculates the subcategories of each causal based on the relationship between the remark and dimension of the incidence of landslides and calculates the landslide sensitivity index (LSI) by adding the frequency ratio of every causal factor.

#### 4.3.2 Landslide Susceptibility Map by using Analytical Hierarchy Processes (AHP)

Landslide hazard assessment involves consideration of several explanatory variables for landslides. Determining the relative contribution of a single parameter in the occurrence of a landslide was a key task. Therefore, the application of the multiple criteria decision method (MCDA) was very important in LHZ mapping technology. The Analytical Hierarchy

Process (AHP) was a multi-standard decision-making process that measures through pairwise comparisons and relies on expert judgment to derive priority scales (Saaty 2008). The analytical hierarchy process operates on four levels, defining problems, determining goals and alternatives, building a paired comparison matrix, determining weights, and obtaining general priorities are four levels, followed by the analytical hierarchy process.

### 4.4 Performance Evaluation of Models

To crosscheck whether the model works properly or not, it is mandatory to do a performance evaluation assessment of the selected models Table 1.

## 5 Discussion

All the factor maps were based on their weight values in the map algebra and produced a landslide susceptibility map using both AHP & FR methods. According to AHP (Table 2), the maximum weight value was recorded at a causative factor of Rainfall and Altitude which are 0.33 and 0.23 respectively followed by Slope (0.16), Lithology (0.11), and Land Use/Cover (0.07) this means that the other causative factors have little or less encouragement for landslide occurrences according to AHP modeling. The landslide susceptibility mapping produced by using AHP methods, which has been classified as very low, low, moderate, high, and very high susceptible zones are strongly correlated with the past landslide inventories. Whereas the landslide susceptibility mapping produced by FR methods for the eight landslide causative factors (Table 1) based on their landslide area relationships with landslide occurrence was calculated. Based on the results of the FR value, the landslide susceptibility mapping was prepared. The landslide susceptibility mapping produced by FR methods shows that 20% very low, 20% low, 21% moderate, 20% high, and 19% of the total study area, shows a very high landslide susceptibility zone (Fig. 8A). Whereas the landslide susceptibility map produced by

**Table 1** Statistical analysis of landslide factors for FR (Abay gorge)

| S/N   | Causals                 | Divisions            | Sub-area % (a) | Observed landslide by % (b) | Value (b/a) |
|-------|-------------------------|----------------------|----------------|-----------------------------|-------------|
| 1     | Slope degree            | 0–10                 | 0              | 0                           | 0.0         |
|       |                         | 10–20                | 30             | 13                          | 0.4         |
|       |                         | 20–30                | 21             | 2                           | 0.1         |
|       |                         | 30–40                | 30             | 25                          | 0.8         |
|       |                         | > 40                 | 18             | 59                          | 3.3         |
|       |                         | Total                | 100            | 100                         | 4.7         |
| 2     | Slope aspect            | Flat                 | 11             | 42                          | 3.9         |
|       |                         | Northeast            | 11             | 4                           | 0.4         |
|       |                         | East                 | 11             | 9                           | 0.8         |
|       |                         | Southeast            | 11             | 4                           | 0.4         |
|       |                         | South                | 11             | 6                           | 0.5         |
|       |                         | Southwest            | 11             | 17                          | 1.5         |
|       |                         | West                 | 12             | 3                           | 0.2         |
|       |                         | Northwest            | 11             | 8                           | 0.8         |
|       |                         | North                | 11             | 7                           | 0.6         |
|       |                         | Total                | 100            | 100                         | 9.1         |
| 3     | Lithology               | Basaltic rocks       | 21             | 11                          | 0.5         |
|       |                         | Sandstone            | 43             | 63                          | 1.5         |
|       |                         | Limestone and gypsum | 22             | 7                           | 0.3         |
|       |                         | Siltstone & Shall    | 14             | 19                          | 1.3         |
|       |                         | Total                | 100            | 100                         | 3.6         |
| 4     | Elevation (m)           | 1030–1368            | 24             | 19                          | 0.8         |
|       |                         | 1368–1603            | 19             | 8                           | 0.4         |
|       |                         | 1603–1848            | 19             | 48                          | 2.5         |
|       |                         | 1848–2168            | 15             | 14                          | 0.9         |
|       |                         | 2168–2451            | 24             | 11                          | 0.5         |
|       |                         | Total                | 100            | 100                         | 5.2         |
| 5     | Distance from road (m)  | 0–200                | 8              | 7                           | 0.9         |
|       |                         | 200–400              | 7              | 2                           | 0.3         |
|       |                         | 400–600              | 7              | 5                           | 0.8         |
|       |                         | 600–800              | 6              | 6                           | 0.9         |
|       |                         | 800–1000             | 12             | 5                           | 0.4         |
|       |                         | 1000–1200            | 11             | 5                           | 0.4         |
|       |                         | 1200–1400            | 11             | 13                          | 1.2         |
|       |                         | > 1400               | 37             | 58                          | 1.5         |
| Total | 100                     | 100                  | 6.4            |                             |             |
| 6     | Distance from stream(m) | 0–100                | 19             | 12                          | 0.6         |
|       |                         | 100–200              | 18             | 9                           | 0.5         |
|       |                         | 200–300              | 17             | 8                           | 0.5         |
|       |                         | 300–400              | 15             | 9                           | 0.6         |
|       |                         | 400–500              | 12             | 8                           | 0.7         |
|       |                         | 500–600              | 10             | 5                           | 0.5         |
|       |                         | > 600                | 8              | 48                          | 0.6         |
| Total | 100                     | 100                  | 9.3            |                             |             |

**Table 1** (continued)

| S/N | Causals        | Divisions          | Sub-area<br>% (a) | Observed<br>landslide by<br>% (b) | Value (b/a) |
|-----|----------------|--------------------|-------------------|-----------------------------------|-------------|
| 7   | Land Use/Cover | Cultivated land    | 94                | 87                                | 0.9         |
|     |                | Forest land        | 1                 | 1                                 | 1.3         |
|     |                | Grass land         | 5                 | 12                                | 2.6         |
|     |                | Shrub land         | 0                 | 0                                 | 0.0         |
|     |                | Waterbodies        | 0                 | 0                                 | 0.0         |
|     |                | Artificial surface | 0                 | 0                                 | 0.0         |
|     |                | Bare land          | 0                 | 0                                 | 0.0         |
|     |                | Total              | 100               | 100                               | 4.8         |
| 8   | Rainfall       | 1214–1232          | 12                | 5                                 | 0.4         |
|     |                | 1232–1250          | 13                | 21                                | 1.6         |
|     |                | 1250–1268          | 75                | 73                                | 1.0         |
|     |                | Total              | 100               | 100                               | 3.0         |

AHP shows that 6% very low, 26% low, 36% moderate, 20% high, and 12% of the total study area is very high landslide susceptibility zone (Fig. 8B).

Landslides are the most dangerous natural hazardous phenomenon that occurred around the world. The current landslide study area, Abay gorge, is continually affected by landslide hazards, especially during the rainy season its frequency is very high due to the fragile nature of the geological materials in the area and topographically suitable for the occurrence of landslides. The reasons for landslides and road failures along the road from Dejen to Renaissance Bridge are too much, the nature of the geological materials, the topography of the area, and improper design of drainage systems in addition to heavy rainfalls and groundwater conditions (Fig. 9A, B). The area is continually at risk of landslides and roadside failures since the geological materials of the area were suitable for the occurrences of landslides, topographically suitable to susceptible/unstable, and poor drainage management systems also lead to the roadside sliding by applying an over-saturated weight on the roadside.

## 6 Conclusions

The main objective of this study was to evaluate and prepare a landslide hazard map in the area from Dejen to Renaissance Bridge, Abay gorge, central Ethiopia. The area is affected by consecutive landslides and roadside failures for the past several decades. Thus, it is very important to evaluate the severity and zonation of the landslide problems in this area. The general methods that followed this study were data collection of the studies for the literature review, detailed field investigation, and preparation of causative factor maps. From this study, it has been founded that the geological nature of the area, due to its fragile and weathered nature, susceptible to sliding as well as the topography of the area were the driving agents of the instability in the area with poor drainage design. Landslide susceptibility maps prepared from FR and AHP models were classified into very low susceptibility, low susceptibility, medium susceptibility, high susceptibility, and very high susceptibility. Both maps show the same and good fitness of present landslide

**Table 2** Pair-wise comparison matrixes of landslide causative factors

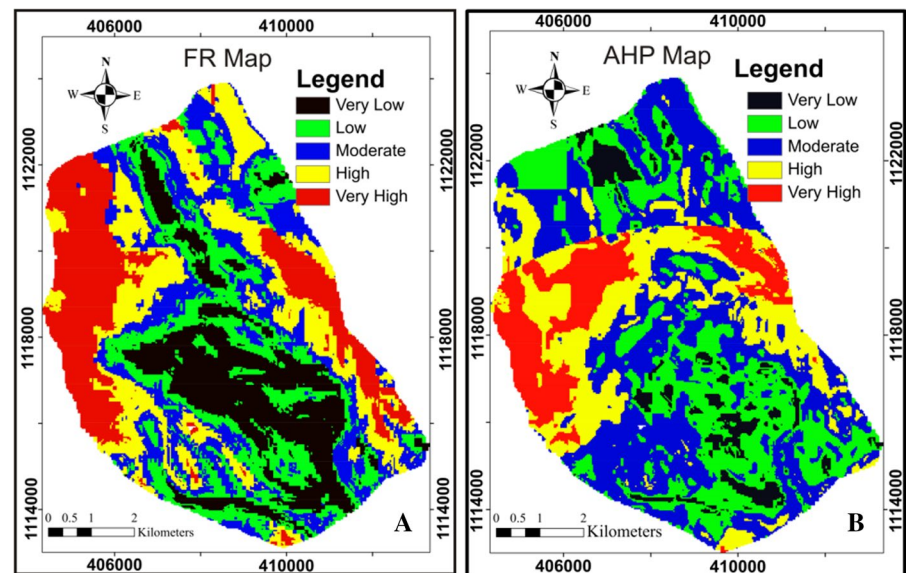
| Class                            | [1] | [2] | [3] | [4] | [5] | [6] | [7] | [8] | Value       |
|----------------------------------|-----|-----|-----|-----|-----|-----|-----|-----|-------------|
| <i>Road proximity</i>            |     |     |     |     |     |     |     |     |             |
| [1] 0–200                        | 1   | 2   | 3   | 4   | 5   | 6   | 7   | 8   | <b>0.32</b> |
| [2] 200–400                      | 1/2 | 1   | 2   | 3   | 4   | 5   | 6   | 7   | <b>0.22</b> |
| [3] 400–600                      | 1/3 | 1/2 | 1   | 3   | 4   | 5   | 6   | 7   | <b>0.18</b> |
| [4] 600–800                      | 1/4 | 1/3 | 1/3 | 1   | 2   | 3   | 4   | 5   | <b>0.10</b> |
| [5] 800–1000                     | 1/5 | 1/4 | 1/4 | 1/2 | 1   | 2   | 2   | 5   | <b>0.07</b> |
| [6] 1000–1200                    | 1/6 | 1/5 | 1/5 | 1/3 | 1/2 | 1   | 2   | 4   | <b>0.05</b> |
| [7] 1200–1400                    | 1/7 | 1/6 | 1/6 | 1/4 | 1/2 | 1/2 | 1   | 2   | <b>0.03</b> |
| [8] > 1400                       | 1/8 | 1/7 | 1/7 | 1/5 | 1/5 | 1/4 | 1/2 | 1   | <b>0.02</b> |
| <i>Geology</i>                   |     |     |     |     |     |     |     |     |             |
| [1] Basaltic Rocks               | 1   | 2   | 3   | 7   |     |     |     |     | <b>0.48</b> |
| [2] Sandstone                    | 1/2 | 1   | 3   | 6   |     |     |     |     | <b>0.33</b> |
| [3] Limestone and Gypsum         | 1/4 | 1/4 | 1   | 5   |     |     |     |     | <b>0.14</b> |
| [4] Siltstone& Shall             | 1/7 | 1/6 | 1/5 | 1   |     |     |     |     | <b>0.05</b> |
| <i>Degree of slope</i>           |     |     |     |     |     |     |     |     |             |
| [1] > 40                         | 1   | 3   | 5   | 6   | 7   |     |     |     | <b>0.49</b> |
| [2] 30–40                        | 1/3 | 1   | 3   | 5   | 7   |     |     |     | <b>0.28</b> |
| [3] 20–30                        | 1/5 | 1/3 | 1   | 2   | 3   |     |     |     | <b>0.11</b> |
| [4] 10–20                        | 1/6 | 1/5 | 1/2 | 1   | 3   |     |     |     | <b>0.08</b> |
| [5] 0–10                         | 1/7 | 1/5 | 1/3 | 1/3 | 1   |     |     |     | <b>0.04</b> |
| <i>Aspect slope</i>              |     |     |     |     |     |     |     |     |             |
| [1] East                         | 1   | 2   | 3   | 4   | 5   | 6   | 7   | 8   | <b>0.32</b> |
| [2] Northeast                    | 1/2 | 1   | 2   | 3   | 5   | 6   | 7   | 8   | <b>0.24</b> |
| [3] Southeast                    | 1/3 | 1/2 | 1   | 2   | 3   | 4   | 5   | 6   | <b>0.15</b> |
| [4] South                        | 1/4 | 1/3 | 1/2 | 1   | 2   | 3   | 4   | 5   | <b>0.11</b> |
| [5] Southwest                    | 1/5 | 1/5 | 1/3 | 1/2 | 1   | 2   | 3   | 4   | <b>0.07</b> |
| [6] West                         | 1/6 | 1/6 | 1/4 | 1/3 | 1/2 | 1   | 2   | 3   | <b>0.05</b> |
| [7] Northwest                    | 1/7 | 1/7 | 1/5 | 1/4 | 1/3 | 1/2 | 1   | 2   | <b>0.03</b> |
| [8] North                        | 1/8 | 1/8 | 1/6 | 1/5 | 1/4 | 1/3 | 1/2 | 1   | <b>0.02</b> |
| <i>Stream proximity (m)</i>      |     |     |     |     |     |     |     |     |             |
| [1] 0–100                        | 1   | 2   | 4   | 5   | 6   | 7   | 8   | 9   | <b>0.35</b> |
| [2] 100–200                      | 1/2 | 1   | 2   | 4   | 5   | 6   | 7   | 8   | <b>0.23</b> |
| [3] 200–300                      | 1/4 | 1/2 | 1   | 3   | 4   | 5   | 6   | 7   | <b>0.15</b> |
| [4] 300–400                      | 1/5 | 1/4 | 1/3 | 1   | 2   | 3   | 4   | 7   | <b>0.10</b> |
| [5] 400–500                      | 1/6 | 1/5 | 1/4 | 1/2 | 1   | 2   | 4   | 5   | <b>0.06</b> |
| [6] 500–600                      | 1/7 | 1/6 | 1/5 | 1/3 | 1/2 | 1   | 3   | 5   | <b>0.05</b> |
| [7] > 600                        | 1/8 | 1/7 | 1/6 | 1/4 | 1/4 | 1/3 | 1   | 3   | <b>0.03</b> |
| <i>Elevation</i>                 |     |     |     |     |     |     |     |     |             |
| [1] 1030–1368                    | 1   | 3   | 5   | 6   | 7   |     |     |     | <b>0.51</b> |
| [2] 1368–1603                    | 1/3 | 1   | 2   | 4   | 5   |     |     |     | <b>0.23</b> |
| [3] 1603–1848                    | 1/5 | 1/2 | 1   | 2   | 3   |     |     |     | <b>0.13</b> |
| [4] 1848–2168                    | 1/6 | 1/4 | 1/2 | 1   | 3   |     |     |     | <b>0.09</b> |
| [5] 2168–2451                    | 1/7 | 1/5 | 1/3 | 1/3 | 1   |     |     |     | <b>0.05</b> |
| <i>Land practice &amp; Cover</i> |     |     |     |     |     |     |     |     |             |
| [1] Cultivated area              | 1   | 2   | 3   | 4   | 6   | 7   | 8   |     | <b>0.37</b> |
| [2] Forestland                   | 1/2 | 1   | 2   | 3   | 4   | 5   | 6   |     | <b>0.23</b> |
| [3] Grass Land                   | 1/3 | 1/2 | 1   | 2   | 3   | 4   | 4   |     | <b>0.15</b> |

**Table 2** (continued)

| Class                  | [1] | [2] | [3] | [4] | [5] | [6] | [7] | [8] | Value       |
|------------------------|-----|-----|-----|-----|-----|-----|-----|-----|-------------|
| [4] Shrub Land         | 1/4 | 1/3 | 1/2 | 1   | 2   | 3   | 3   |     | <b>0.10</b> |
| [5] Water Bodies       | 1/6 | 1/4 | 1/3 | 1/2 | 1   | 2   | 2   |     | <b>0.07</b> |
| [6] Artificial Surface | 1/7 | 1/5 | 1/4 | 1/3 | 1/2 | 1   | 2   |     | <b>0.05</b> |
| [7] Bare Land          | 1/8 | 1/6 | 1/4 | 1/3 | 1/2 | 1/2 | 1   |     | <b>0.04</b> |
| <i>Rainfall</i>        |     |     |     |     |     |     |     |     |             |
| [1] 1250–1268          | 1   | 3   | 7   |     |     |     |     |     | <b>0.64</b> |
| [2] 1232–1250          | 1/3 | 1   | 5   |     |     |     |     |     | <b>0.28</b> |
| [3] 1214–1232          | 1/7 | 1/5 | 1   |     |     |     |     |     | <b>0.07</b> |

The significance of bold is the weight value of each sub-class

**Fig. 8** LSM map produced using **A** FR and **B** AHP Methods



locations so this is very important for the prediction of future landslide locations in the area. Landslide density increases from low to very high susceptibility class in both models.

The results from the final map evaluations indicate that 99% of landslide data fall in the high susceptibility and very high susceptibility ranges. Therefore, the maps produced can prove to be reliable and helpful in the landslide risk assessment and can guide planners in the implementation of developmental projects at safer locations and or to take any action of mitigations for a reduction in the landslide areas based on the recommendations of the result. Based on the

findings of the study the following recommendations are forwarded:—(1) Construct appropriate and suitable drainage structures on the side of the roads. (2) Recommending retaining structures on the critical slope sections. (3) Support unstable slope sections with bioengineering activities. (4) drain the streams in the area in a proper manner to reduce the toe erosion and add loads on the sliding materials. Generally, an integrated approach of remedial measures may be helpful to minimize the effects and occurrence of landslide hazards in the area. In addition, land use planning and land use management studies should be done for further landslide-prone areas.



**Fig. 9** The figures, show maintenance of the **A** roadside slide, and **B** Road slides

**Acknowledgements** My deepest gratitude is going to the local people of Dejen, Kurare, and the surrounding areas for their honesty and hospitality during my fieldwork. I would like to thank the anonymous reviewers for their constructive comments and suggestions on the manuscript and last but not least to Mr. Alehegn W., Dr. Getnet B., Dr. Ayenew M., Dr. Getachew M., and Mr. Asenake T. for their remarkable contribution to this work.

**Funding** There is no funding source for this work.

#### Declarations

**Conflicts of interest** I am delighted to submit the manuscript, Landslide Hazard Evaluation and Zonation in the Abay Gorge, along with the Road section from Dejen–Renaissance Bridge, Ethiopia, I declare that no conflicts of interest associated with this publication, and there was no significant financial support for this work that could have influenced its outcome. As Corresponding Author, I, as a result of this, confirm that the author declares that no competing interests.

#### References

Asmare D, Tesfa C (2022) Application and validation of the evaluation using slope stability susceptibility evaluation parameter rating system to debre werk area (Northwest Ethiopia). *Geotech Geol Eng* 40:1–14

- Ayalew L, Yamagishi H (2005) The application of GIS-based logistic regression for landslide susceptibility mapping in the Kakuda-Yahiko mountains, Central Japan. *Geomorphology* 65:15–31
- Barsch D, Caine N (1984) The nature of mountain geomorphology. *Mt Res Dev* 4:287–298
- Brunsdon D, Thornes J (1979) Landscape sensitivity and change. *Trans Inst Br Geogr* 4:463–484
- Cruden DM (1991) A simple definition of a landslide. *Bull Int Assoc Eng Geol-Bull De L' Assoc Int De Géologie De L'ingénieur* 43:27–29
- Dahoua L, Yakovitch SV, Hadji R, Farid Z (2017a) Landslide susceptibility mapping using analytic hierarchy process method in BBA-Bouira Region, case study of East-West Highway, NE Algeria. In: Kallel A, Ksibi M, Dhia HB, Khélifi N (eds) *Euro-mediterranean conference for environmental Integration*. Springer International Publishing, Cham, pp 1837–1840. [https://doi.org/10.1007/978-3-319-70548-4\\_532](https://doi.org/10.1007/978-3-319-70548-4_532)
- Dahoua L, Yakovitch SV, Hadji RH (2017b) GIS-based technic for roadside-slope stability assessment: an bivariate approach for A1 East-west highway, North Algeria. *Min Sci* 24:117–127
- Dai F, Lee C, Ngai YY (2002) Landslide risk assessment and management: an overview. *Eng Geol* 64:65–87
- Das S, Sarkar S, Kanungo DP (2022) GIS-based landslide susceptibility zonation mapping using the analytic hierarchy process (AHP) method in parts of Kalimpong Region of Darjeeling Himalaya. *Environ Monit Assess* 194:1–28
- El Mekki A, Hadji RL, Chemseddine F (2017) Use of slope failures inventory and climatic data for landslide susceptibility, vulnerability, and risk mapping in souk Ahras region. *Min Sci* 24:237–249
- Gautam P, Kubota T, Sapkota LM, Shinohara Y (2021) Landslide susceptibility mapping with GIS in high mountain area of Nepal: a comparison of four methods. *Environ Earth Sci* 80:1–18
- Hadji R, Limani Y, Baghem M, Demdoum A (2013) Geological, topographic and climatic controls in landslide hazard assessment using GIS modeling: a case study of Souk Ahras region, NE Algeria. *Quatern Int* 302:224–237
- Hadji R, Limani Y, Demdoum A (2014) Using multivariate approach and GIS applications to predict slope instability hazard case study of Machrouha municipality, NE Algeria. In: 2014 1st International conference on information and communication technologies for disaster management (ICT-DM), IEEE, pp 1–10
- Hagos AA (2013) Remote sensing and GIS-based mapping on landslide phenomena and landslide susceptibility evaluation of Debresina Area (Ethiopia) and Rio San Girolamo basin (Sardinia)
- Hamad A, Hadji R, Bâali F, Houda B, Redhaounia B, Zighmi K, Legrioui R, Brahmi S, Hamed Y (2018) Conceptual model for karstic aquifers by combined analysis of GIS, chemical, thermal, and isotopic tools in Tuniso-Algerian transboundary basin. *Arab J Geosci* 11:1–16
- Hamza T, Raghuvanshi TK (2017) GIS based landslide hazard evaluation and zonation—a case from Jeldu District, central Ethiopia. *J King Saud Univ Sci* 29:151–165
- Lee S (2005) Application of logistic regression model and its validation for landslide susceptibility mapping using GIS and remote sensing data. *Int J Remote Sens* 26:1477–1491

- Manchar N, Benabbas C, Hadji R, Bouaicha F, Grecu F (2018) Landslide susceptibility assessment in Constantine region (NE Algeria) by means of statistical models. *Studia Geotech Et Mech* 40:208–219
- Mersha T, Meten M (2020) GIS-based landslide susceptibility mapping and assessment using bivariate statistical methods in Simada area, northwestern Ethiopia. *Geoenviron Disasters* 7:1–22
- Mittal S, Singh M, Kapur P, Sharma B, Shamshi M (2008) Design and development of instrumentation for landslide monitoring and issue. *J Sci Ind Res (JSIR)* 67:361–365
- Roccati A, Paliaga G, Luino F, Faccini F, Turconi L (2021) GIS-based landslide susceptibility mapping for land use planning and risk assessment. *Land* 10:162
- Saaty TL (2000) Fundamentals of decision making and priority theory with the analytic hierarchy process. RWS Publications, Pittsburgh
- Saaty TL (2008) Decision making with the analytic hierarchy process. *Int J Serv Sci* 1:83–98
- Salehpour Jam A, Mosaffaie J, Sarfaraz F, Shadfar S, Akhtari R (2021) GIS-based landslide susceptibility mapping using hybrid MCDM models. *Nat Hazards* 108:1025–1046
- Solaimani K, Mousavi SZ, Kavian A (2013) Landslide susceptibility mapping based on frequency ratio and logistic regression models. *Arab J Geosci* 6:2557–2569
- Tang R-X, Kulatilake PH, Yan E, Cai J-S (2020) Evaluating landslide susceptibility based on cluster analysis, probabilistic methods, and artificial neural networks. *Bull Eng Geol Env* 79:2235–2254
- Tesfa C, Woldearegay K (2021) Characteristics and susceptibility zonation of landslides in Wabe Shebelle Gorge, south eastern Ethiopia. *J Afr Earth Sc* 182:104275
- Varnes DJ (1984) Landslide hazard zonation: a review of principles and practice. United Nations, San Francisco
- Voogd H (1988) Multicriteria evaluation: measures, manipulation, and meaning—a reply. *Environ Plan B Plan Design* 15:65–72
- Woldearegay K (2013) Review of the occurrences and influencing factors of landslides in the highlands of Ethiopia: with implications for infrastructural development. *Momona Ethiopian J Sci* 5:3–31
- Ye C-M, Wei R-L, Ge Y-G, Li Y, Junior JM, Li J (2022) GIS-based spatial prediction of landslide using road factors and random forest for Sichuan-Tibet highway. *J Mt Sci* 19:461–476
- Zhao P, Masoumi Z, Kalantari M, Aflaki M, Mansourian A (2022) A GIS-based landslide susceptibility mapping and variable importance analysis using artificial intelligent training-based methods. *Remote Sens* 14:211

**Publisher's Note** Springer Nature remains neutral with regard to jurisdictional claims in published maps and institutional affiliations.